

Auto-ML Deep Learning for Rashi Scripts OCR

Shahar Mahpod, Yosi Keller

Abstract—In this work we propose an OCR scheme for manuscripts printed in Rashi font that is an ancient Hebrew font and corresponding dialect used in religious Jewish literature, for more than 600 years. The proposed scheme utilizes a convolution neural network (CNN) for visual inference and Long-Short Term Memory (LSTM) to learn the Rashi scripts dialect. In particular, we derive an AutoML scheme to optimize the CNN architecture, and a book-specific CNN training to improve the OCR accuracy. The proposed scheme achieved an accuracy of more than 99.8% using a dataset of more than 3M annotated letters from the Responsa Project dataset.

I. INTRODUCTION

The Optical Character Recognition (OCR) of printed media such as books and newspapers is of major importance, as it enables digital access, archiving, search and Natural Language Processing (NLP) based analysis of texts. A gamut of digitization projects, such as the America’s Historical Newspapers, 1690-1922¹, the California Digital Newspaper Collection², the Doria project, and the digitization Project of Kindred Languages³, to name a few, were established. Some OCR projects deal with Hebrew language digitization, such as the Historical Jewish Press project⁴, and the Early Hebrew Newspapers Project⁵, while others, such as the Responsa Project⁶, Historical Dictionary Project⁷, Otzar HaHochma⁸ and HebrewBooks⁹, focus on religious Jewish literature. It is common in such projects to utilize commercial OCR packages such as ABBYY¹⁰ or OmniPage¹¹.

Faculty of Engineering, Bar Ilan University, Israel. mahpod.shahar@gmail.com.

Faculty of Engineering, Bar Ilan University, Israel. yosi.keller@gmail.com.

¹<http://www.readex.com>

²<http://cdnc.ucr.edu/cgi-bin/cdnc>

³<http://www.doria.fi>

⁴<http://web.nli.org.il/sites/JPress/Hebrew/Pages/default.aspx>

⁵<http://jnul.huji.ac.il/dl/newspapers/index1024.html>

⁶<http://www.responsa.co.il>

⁷hebrew-treasures.huji.ac.il

⁸<http://www.otzar.org/wotzar>

⁹<http://hebrewbooks.org/>

¹⁰<https://www.abbyy.com/>

¹¹<http://www.nuance.com/for-individuals/by-product/omnipage/index.htm>

The Responsa Project is one of the largest scale digitizations of Hebrew and Jewish books. In particular, it specializes in Rashi script OCR that is an ancient typeface of the Hebrew alphabet, based on a 15th century Sephardic semi-cursive handwriting. It has been used extensively in Jewish religious literature and Judaeo-Spanish books for more than 600 years, and is in large scale use nowadays. Rashi and Hebrew scripts letters are depicted in Table I. We denote as *characters* the different manifestations (in different fonts) of the same underlying *letters*.

Pattern Matching [1] and Feature Extraction [2], [3] were applied to OCR, by comparing series of image descriptors encoding the characters, such as SIFT [2], SURF [4], and PCA [3] to name a few. The recognition was formulated as a classification task using SVM [3], [2]. OCR was one of the first applications of Convolutional Neural Networks (CNNs), due to the seminal work by LeCun et al. [5].

The recognition accuracy of OCR can be improved by applying NLP to the visual analysis results. NLP was applied using dictionaries [6], [7], statistical algorithms such as HMM [8], Graph optimization [9] and LSTM [10]. Contemporary CNN-based NLP schemes often utilize word embeddings [11], alongside RNN and LSTM layers. The work of Kim et al. [12], is of particular interest as multiple stacked LSTM layers were used to compute a hierarchy of embeddings, first embedding the sequence of letters to represent words, and the sequence of words to represent sentences.

In this work we study the OCR of Rashi scripts that entails several challenges. First, being an exotic font, there are no commercial or academic OCR softwares for creating a training set. Second, it is common in some books to utilize the Rashi font as a primary font, alongside regular printed Hebrew fonts to emphasize the beginning of paragraphs, as shown in Fig. 1, or mark citations from older books, such as the Bible or the Talmud.

Third, the Rashi script books were printed by different printing houses, over more than 500 years, resulting in significant variations of the script, as depicted in Fig. 2.

א	ב	ג	ד	ה
alf	bet	gml	dlt	hea
ו	ז	ח	ט	י
vav	zin	het	tet	yod
ך	כ	ל	ם	מ
kaf-p	kaf	lmd	mem-p	mem
ן	נ	ס	ע	ף
nun-p	nun	smk	ain	peh-p
פ	ץ	צ	ק	ר
peh	zdk-p	zdk	kuf	rsh
ש	ת			
shn	tav			

TABLE I

PRINTED HEBREW CHARACTERS AND THE CORRESPONDING RASHI CHARACTERS. THE LEFT CHARACTER IN EACH CELL IS THE PRINTED HEBREW CHARACTER, WHILE THE RIGHT CHARACTER IS THE CORRESPONDING RASHI CHARACTER.

לכך לפענ"ד הנכון דעה התוספת בסנהדרין דף ג'
הג"ל, דרובא דלדיא לא חשיב רוב גמור אצל
רוב גמור אף ד"מ מהני. ונראה ביאור דצריהם פשוט
וכן ראיתי בצ"ח צה"מ סימן רל"ב, משום שכנגד אדם
אחד שקונה מאה שורים לדיא, איכא מאה בני אדם
שקונים עשרה שורים לאכילה, ואיכא רוב לוקחים

Fig. 1. An example of a Rashi script manuscript. Part of a manuscript printed in Rashi script, taken from "Shut Rabeynu Yosef Mislutsk" manuscript, printed in Slutsk (Belarus), at the first half of the 19 century.

For instance, the pair of different characters {'ain','tet'}, {'dlt','rsh'}, {'nun-p','zdk-p'} are similar, while the same letters printed by different printing houses might look different, as depicted in Fig. 3.

Other issues relate to handling scanning effects such as impurities, skewed text lines, and page folds as depicted in Figs. 4 and 5.

Some ancient Jewish books are fully or partially written in Aramaic language, contain special symbols for acronyms, and a rare composition of א (alf) and ל (lmd) as in Fig. 6. Implying that the OCR schemes can not apply standard dictionaries and spelling correction schemes, that have to be learnt as part of the OCR scheme. As the Rashi script consists of disconnected

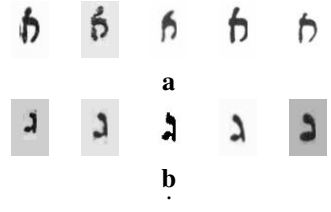


Fig. 2. The variability in Rashi script letters appearing in different books. (a) Samples of the letter א (alf). (b) Samples of the letter ג (gml).

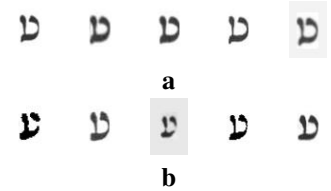


Fig. 3. The visual similarity of different letters. (a) The letter ט (tet) is visually similar to (b) ע (ain).

characters, the agnostic detection of isolated characters, that is the detection of the bounding box of each character without detecting the character's class, can be easily implemented.

In this work we propose a Deep Learning based OCR scheme for learning both the visual representation of the Rashi script, and the spelling of the corresponding manuscripts. This is a particular example of scripts in an exotic language, where both the font and spelling are apriori unknown. The proposed scheme is fully data driven and does not utilize predefined dictionaries. We

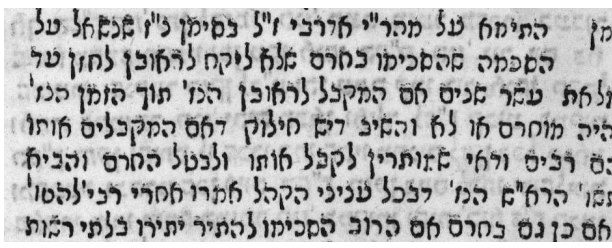


Fig. 4. An example of a corrupted manuscript page scanned from the book "Pney Aharon", printed in Saloniki, Greece, at the first half of the 18th century.



Fig. 5. Examples of corrupted and distorted Rashi script letters scanned in different books. The top line shows the samples of the letter א (alf), while the bottom line depicts the letter ג (gml).



Fig. 6. Special and rare symbols in Rashi scripts. This special symbol combines the letters \aleph (alf) and \beth (lmd).

derive a unified Deep network that combines a CNN to visually classify the characters, with a LSTM to learn the corresponding spelling, and thus improve the OCR accuracy.

In particular, we propose the following contributions:

First, we derive a Deep network consisting of a CNN trained over 3M Rashi script samples, and a LSTM layer trained over words, that is shown to yield highly accurate OCR results.

Second, we derive an Auto-ML scheme based on Genetic Algorithms to optimally design the structure of the CNN. This results in an improved OCR accuracy achieved by a CNN three-fold smaller.

Last, we propose an active learning approach for refining the net accuracy when applied to a particular book, by refining the CNN model using a small set of the test characters.

The rest of this paper is organized as follows: we start by reviewing previous works on deep learning based OCR in Section II. The proposed approach is introduced in Section III, while the experimental validation and comparison between different schemes is presented in Section IV. Concluding remarks and future work are discussed in Section V.

II. RELATED WORK

Optical Character Recognition (OCR) is a common task in computer vision, used in a gamut of applications and languages such as, English [13][14], Chinese [15] and Japanese [16]. The OCR of exotic languages such as the Rashi script is less applicative and common.

Similar to our work, Deep Learning (DL) was applied to exotic languages. A LeNet-based CNN [17] was applied by Rakesh et al. [18] for the OCR of the Telugu script consisting of ~ 460 symbols that were encoded by binary image patches. A similar architecture was applied by Kim et al. [19] for the OCR of the handwritten Hangul script, while using the MSE as a loss function. A weighted MSE was proposed to handle the imbalanced training set during training.

A deep belief network (DBN), with three fully connected layers, was proposed by Sazal et al. [20] for the Bangla handwritten OCR dataset consisting of ten numerals and 50 characters. The layers were initialized using a restricted Boltzmann machine (RBM), and a

softmax loss was used to classify the characters. A similar approach was applied by Ma et al. [21] for the OCR of a Tibetan script consisting of 562 characters and applied a three-layers DBM initialized using a RBM. SIFT local image descriptors were applied by Sushma and Veena [22] to encode and detect the characters of the Kannada language that uses 49 phonemic characters, where different characters can be composed to encode a single symbol. A Hidden Markov Model (HMM) was applied to improve the decoding of the language symbols by training the HMM using texts.

Deeper CNNs were used by Zhong et al. [23] for the Handwritten Chinese Character Recognition (HCCR) competition, by considering AlexNet [24] and GoogLeNet [25], where the images of the characters, their image gradients, HOG and Gabor descriptors were used as features. Stacked RNNs, the first for script identification and the second for recognition were applied by Mathew et al. [26] to the OCR of multilingual Indic Scripts, such as the Kannada, Bangla, Telugu and other languages. Both networks consisted of three hidden layers and a LSTM layer. Fuzzy logic and spatial image statistics were used by Gur and Zelavsky [27] to recognize distorted letters by using the combination of letter statistics and correlation coefficients.

OCR is a particular example of the Structured Image Classification problem where the classification problem is hierarchial. Such that the lower layers analyze the visual data, and the succeeding layers analyze the inner (semantic) structure of the data. In the proposed OCR scheme, the lower inference layer is implemented by a CNN that classifies the visual manifestations of the characters, and the semantic inference sub-network learns the particular dialect used in Rashi scripts using LSTM. A Structured Image Classification problem was studied by Goldman and Goldberger [28] in the context of structured object detection, where rows of products are detected in images by a CNN-based object detection scheme. The order (structure) of the detected objects is learnt by embedding the indexes of triplets of neighboring objects by an embedding layer, and concatenating the structure embeddings with the Fully Connected (FC) layer of the object detector. The resulting vector is used to infer the true label of the input image. In contrast, the proposed scheme processes a *sequence* of object images simultaneously, and the sequential data is encoded by a LSTM layer. Bar et al. detect compression fractures in CT scans [29] of the human spine. The spine that is a linear structure, was first segmented, and its corresponding patches were binary classified using a CNN. Recurrent Neural Network (RNN) was used to predict the existence of a fracture. Our proposed scheme infers

multiple labels both by the CNN layers (characters) and LSTM (words).

III. OCR OF RASHI SCRIPTS USING DEEP LEARNING

We study the OCR of Rashi scripts where the locations of the characters are initially detected. Hence, the OCR is formulated as a classification problem, where given a sequence of images of characters $\{\phi_1, \dots, \phi_J\}$, we aim to classify $C(\phi_j) \in \{c_1, \dots, c_L\}$, that are the latent character labels. We utilize a Deep Learning scheme consisting of two stacked sub-networks. The initial one, is a CNN that computes the detection probabilities of the characters based on the input images, while the succeeding sub-network utilizes a LSTM layer to improve the decoding accuracy, by learning a data-driven vocabulary. An overall view of the proposed scheme is depicted in Fig. 7.

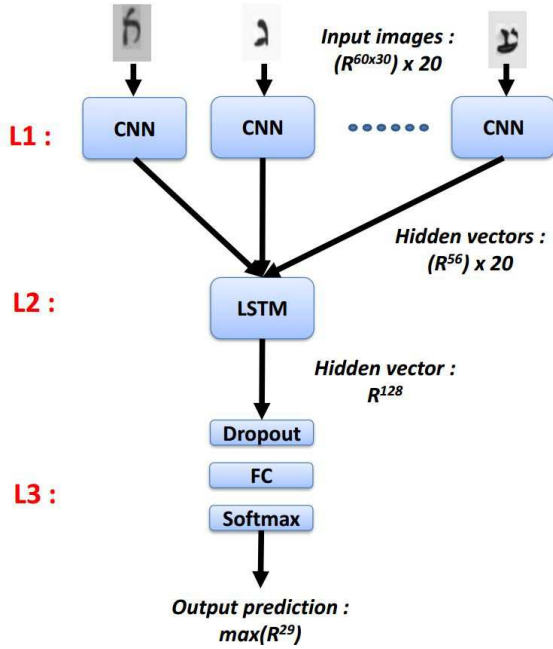


Fig. 7. The proposed OCR scheme, consisting of the CNN (L1) that classifies the characters' images and outputs prediction probabilities per class, while the LSTM (L2) agglomerates the probabilistic characters detections into words and sentences.

We studied several CNN architectures for classifying the images of the detected characters. The first denoted Simple NN (SNN) is based on the LeNet5 architecture [17] detailed in Table II.

Following the work of Zhong et al.[23], we also applied a deeper CNN based on AlexNet [24], detailed in Table III.

The Spatial Transformer layer [30][31] was shown to improve OCR accuracy, by geometrically rectifying

Layer	Type	Parameters	Stride
L01	conv	[5 5 1]x20	
	max pool	[2 2]	[2]
L02	conv	[5 5 20]x50	
	max pool	[2 2]	[2]
L03	conv	[4 4 50]x500	
	max pool	[2 1]	[4 1]
L04	conv	[2 1 50]x500	
	relu		
L05	conv	[1 1 500]x56	
	softmax		

TABLE II

THE CNN USED FOR VISUAL CLASSIFICATION OF THE CHARACTERS, BASED ON THE LeNET5 CNN [17].

Layer	Type	Parameters	Stride
L01	conv	[11 11 1]x96	[2 1]
	bnorm		
	relu		
L02	max pool	[3 3]	[2]
	conv	[5 5 48]x256	
	bnorm		
L03	max pool	[3 3]	
	conv	[3 3 256]x384	
	bnorm		
L04	conv	[3 3 384]x192	
	bnorm		
	relu		
L05	conv	[3 3 192]x256	
	bnorm		
	relu		
L06	max pool	[3 3]	
	conv	[6 6 256]x4096	
	bnorm		
L07	conv	[1 1 4096]x4096	
	bnorm		
	relu		
L08	conv	[1 1 4096]x56	
	softmax		

TABLE III

THE CNN USED FOR VISUAL CLASSIFICATION OF THE CHARACTERS, BASED ON THE ALEXNET ARCHITECTURE [24].

the input image by estimating the underlying affine transformation. Thus, we added the Spatial Transformer layer to the MNIST CNN, and denote the resulting CNN Spatial Transformer Net (STN), as reported in Table IV.

Thus, the output of the CNN is the classification probabilities, $\{p_{j,l}\}_{1,1}^{J,L}$ of the input sequence of character images $\{\phi_j\}_1^J$, such that $p_{j,l}$ is the *estimated* probability of an image $\phi_j \in \{\phi_j\}_1^J$ to be related to the class (letter) $c_l \in \{c_l\}_1^L$. As a script might contain both Rashi and printed Hebrew fonts, we set $L = 56$, consisting of 27 characters of Rashi script, 27 characters of Printed Hebrew script, one for a special character 'a-l' and a single space character.

Layer	Type	Parameters	Stride
	max pool	[2 2]	[2 1]
L01	conv	[5 5 1]x20	
	relu		
	max pool	[2 2]	[2]
L02	conv	[5 5 20]x20	
	relu		
L03	conv	[9 9 20]x50	
	relu		
L04	conv	[1 1 50]x6	
	grid		
	sampler		
	max pool	[2 2]	
L05	conv	[7 7 1]x32	
	relu		
	max pool	[2 2]	[2]
L06	conv	[7 7 1]x32	
	relu		
	max pool	[2 2]	[2]
L07	conv	[4 4 32]x48	
	relu		
	max pool	[2 2]	[2]
L08	conv	[4 4 48]x256	
	relu		
L09	conv	[1 1 256]x56	
	softmax		

TABLE IV
THE CNN USED FOR VISUAL CLASSIFICATION OF THE CHARACTERS BASED ON THE MNIST CNN AND A SPATIAL TRANSFORMER LAYER [30].

The scripts are written in a particular Hebrew dialect that can be utilized to better infer the estimated symbols, as being part of words and sentences. For that we apply Long-short term memory (LSTM) [32] that allows to encode and utilize the inherent sequential information. The LSTM layer is denoted as $L2$ in Fig. 7 and consists of 20 memory units, where the input to each LSTM module is $\{p_{j,l}\}_1^L \in R^{56}$, (20 vectors in total), and the output in R^{128} encodes the sequence of CNN outputs $\{p_{j,l}\}_{1,1}^{J,L}$.

A. AutoML CNN architecture refinement using a genetic algorithm

We applied AutoML to refine the CNNs proposed in Section III by optimizing the classification accuracy with respect to the CNN architecture, that is given by the parameters of its layers. In particular, we consider a CNN similar to LeNet5 [17] consisting of sequential pairs of convolution and activation layers that are jointly optimized. Thus, we optimize the parameters of the convolution layers: the support of the filter, the number of filters (output dimensionality), the stride in both image axes, the use of batch normalization, and the use of a dropout layer and its probability. The activation layer is given by its type (ReLU, Avg-Pool, Max-Pool), where

the pooling layers are given by their pooling support and stride.

AutoML is a nonlinear optimization over a heterogeneous set of discrete (filters support, stride etc.) categorical (activation type) and continuous (dropout rate) parameters. For that we apply a Genetic Algorithm (GA) [33] by first (generation $g = 0$) drawing $N = 120$ random CNNs $\{CNN_i^{g=0}\}$ similar to LeNet5, each consisting of l convolution+activation layers, followed by a fixed FC layer. Each such CNN is trained for $M = 10$ epochs using $\sim 5\%$ of the training data. The K_1 CNNs having the highest validation accuracy are denoted as the *Elite* set, while $P = 40\%$ of the remaining CNNs with the highest validation accuracy are denoted as *Parents*.

The next generation of CNNs $\{CNN_i^{g+1}\}$ is derived by computing *Children*, *Mutations*, and *Random* CNNs: *Children* are computed by randomly picking pairs of *Parents* CNNs and splitting each of them randomly, and connecting the resulting sub-CNNs, that are of varying lengths $\{l_n\}_1^N$. *Mutations* are created by picking a random parent and randomly changing a single CNN parameter. Additional *Random* CNNs are drawn as in the initialization phase. Thus, $\{CNN_i^{g+1}\}$ is initialized by propagating the *Elite* set to $\{CNN_i^{g+1}\}$, and adding the K_2 CNNs in $\{Children \cup Mutations \cup Random\}$ having the highest validation accuracy

$$\{CNN_i^{g+1}\} = \underset{K_2}{Elite} \cup \max \{Children \cup Mutations \cup Random\}. \quad (1)$$

This scheme is summarized in Algorithm 1, and was applied to generate multiple consecutive generations. It is initialized by running Algorithm 1 for $l = \{3, 5, 7, 9\}$ and selecting the resulting CNNs having the highest validation accuracy. Algorithm 1 is then applied to this set of CNNs, and the resulting CNN is shown in Table V.

B. Book specific OCR-CNN refinement

A particular attribute of the Rashi scriptures is that their Hebrew dialect was and still is a sacred religious dialect and was not in daily use, as the scholars using it lived in non-Hebrew speaking countries: Europe, North Africa, etc. Thus, it did not undergo significant changes in 600 years, and over different geographical regions. Hence, most Rashi manuscripts share a similar dialect and vocabulary, but might differ in the graphical printing

Algorithm 1: AutoML for CNN optimization using a Genetic Algorithm

- 1:
 - 2: **Initialization:** Generate N random CNNs $\{CNN_i^{g=0}\}$ having l convolution+activation layers.
 - 3: **for** $g < G$ **do**
 - 4: Train $\{CNN_i^g\}$ for M epochs
 - 5: Apply $\{CNN_i^g\}$ on the validation set V
 - 6: $Elite = \max_{K_1} \{CNN_i^g(V)\}$
 - 7: Compute the *Children*, *Mutations*, and *Random* sets of CNNs based on V .
 - 8: $\{CNN_i^{g+1}\} = Elite \cup \max_{K_2} \{Children \cup Mutations \cup Random\}$
 - 9: **end for**
-

Layer	Type	Parameters	Stride
L01	conv	[7 7 1]x19	[1 2]
	dropout		
	avg pool	[4 2]	
L02	conv	[7 1 19]x83	
	max pool	[4 3]	[3 1]
L03	conv	[14 9 83]x987	[14 9]
	relu		
L04	conv	[1 1 987]x56	
	softmax		

TABLE V
THE OCR CNN (L1 IN FIG. 7) COMPUTED BY APPLYING THE AUTOML SCHEME.

attributes of the Rashi script, when printed by different printing houses, as depicted in Fig. 2.

In order to utilize the dialect invariance, in contrast to the varying graphical manifestation of the Rashi script letters, we propose to refine the CNN *per script* while freezing the LSTM layer, and use the *test* classifications as a training set for refining the CNN. For that, given a test manuscript, we apply the CNN+LSTM as in Section III, to $\sim 5\%$ of the new script, and utilize the OCR output as a training set for refining the CNN. The resulting CNN is applied to the rest of the manuscript.

IV. EXPERIMENTAL RESULTS

In this section we experimentally verify the validity and accuracy of the proposed scheme by applying it to a large dataset provided by the Responsa project consisting of ~ 2500 pages extracted from 170 different books. The dataset contains 5.5M annotated letters given their positions and labels. There are on average 3400 letters per page, where some of the manuscripts contain several pages, while others more than 20 pages. The images of the letters are of size of 60x30 pixels, and their distribution is depicted in Fig. 8.

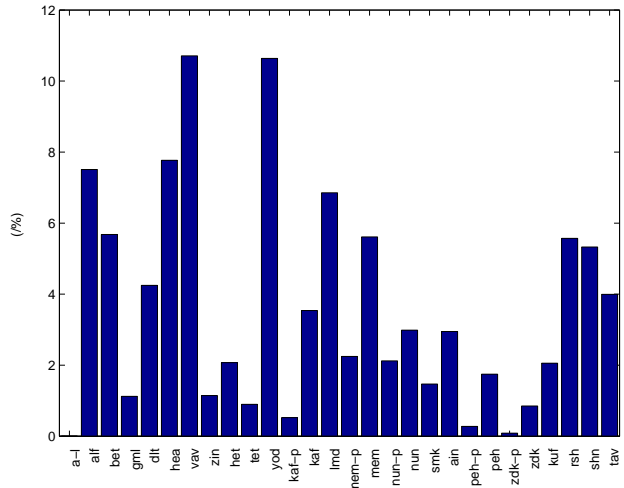


Fig. 8. The distribution of letters in the Responsa project dataset for both Printed and Rashi scripts.

We divided the Responsa project dataset into three sets S^r , S^v and S^t consisting of 3.3M, 352K, and 2M letters, respectively. S^r is the training set consisting of 140 books and more than 1000 pages. S^v was the validation set (114 pages from 15 books), and S^t was the testing set collected from other 15 books. The test set S^t was divided into two subsets $S^t = S_1^t \cup S_2^t$, where S_1^t consists of the first 40K letters in each book, while the set S_2^t comprises of the remaining letters in a manuscript, 1.35M letters overall. S_1^t was used for the book-specific CNN refinement scheme introduced in Section III-B, while S_2^t was used as a test set.

We applied the CNNs detailed in Section III and the CNN computed using the AutoML scheme introduced in Section III-A, for which we used 2% of the samples in the set S^r and 10% of S^v , 75K and 35K letters, respectively. The AutoML refinement was applied using seven different initial 'families', each was trained for $G = 10$ generations and 120 mutations each. The number of convolution layers, the activations succeeding each convolution layer (ReLU, Max-Pool or Avg-Pool), and the addition of batch normalization or dropout layers are randomly drawn. Similarly, the layers' parameters (filters sizes, max pooling size, stride value and dropout percentage) are also randomly drawn. The families differ by the maximal number of initial layers.

Other than the first generation, all of the mutations were chosen randomly, the succeeding generations were composed of $K_1 = 5$ Elite group, 70 Cross-Over children and 25 mutations of the parents. The group of parents was collected from the $K_2 = 40$ most accurate CNNs (including the Elite group) computed in the pre-

vious generation. We also added additional 20 random mutations at each generation to increase the variability. The Elite group from the last generation of each family is gathered into a single set of CNNs and refined for $G = 10$ generations and 120 mutations. Figure 9 depicts the average classification error reduction with respect to the number of training AutoML generations.

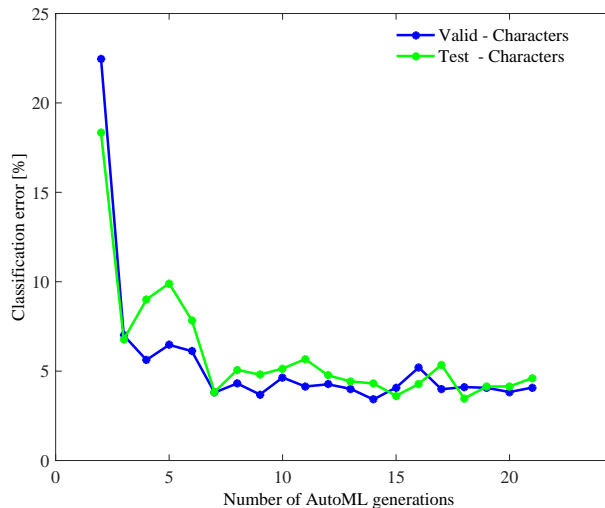


Fig. 9. The classification accuracy of the AutoML optimized CNN with respect to the Genetic Algorithm’s refinement iterations.

A. OCR results using AutoML CNN

We start by evaluating the proposed OCR scheme accuracy of the four CNNs introduced in Section III, *without* the additional accuracy of the LSTM layer. The accuracy of the overall scheme (CNN+LSTM) is discussed in Section IV-B. Figure 10 reports the classifications accuracy of the CNNs with respect to the size of training set S^r . For each CNN we consider the accuracy of detecting the 56 graphical symbols denoted as *Characters*, and the accuracy of detecting the set of 29 *phonetic* equivalents as *Letters*, where each *Letter* (other than ‘space’ and punctuation marks) can be mapped to two *Characters*, in Rashi and Printed fonts. The accuracy results are also reported in Table VI, where it follows that the SNN (based on the LeNet5 CNN) is inferior to the deeper AlexNet-based ALX and STN CNNs. The Spatial Transformer layer does not improve the accuracy significantly compared to AlexNet, and we attribute that to the deskewing of the OCR input images applied in the preprocessing phase, such that the additional rectification of the Spatial Transformer layer is insignificant.

The accuracy gap between the *Characters* and *Letters* is due to the similarity in Rashi and Printed *Characters*

of some of the letters, as depicted in Table I. Thus, the CNNs might misclassify some character images as being Rashi instead of Printed and vice versa, while relating to the same *Letter*. This is considered a *Character* classification error, and a correct *Letter* classification. The proposed AutoML scheme is shown to significantly outperform all other schemes while utilizing the least number of the CNN parameters.

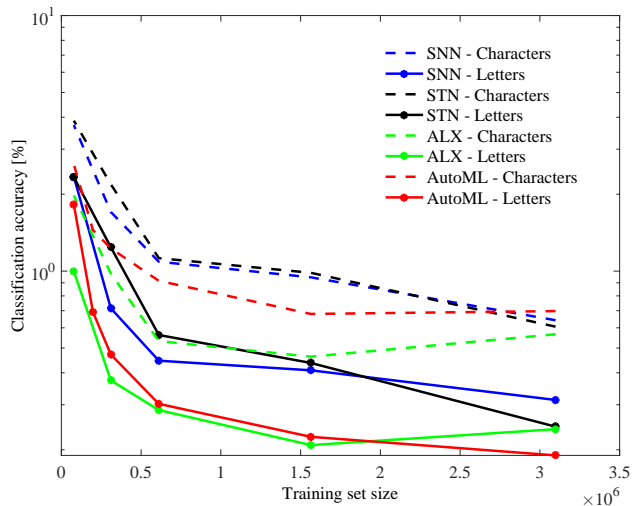


Fig. 10. The Characters and Letters classification accuracy of the proposed CNNs, with respect to the training set size. STN - Spatial transform net. ALX - AlexNet. AutoML - optimized by a Genetic Algorithm.

Scheme	Error rate [%]	Number of CNN Parameters
SNN	0.313	1.01M
STN	0.243	0.73M
AlexNet	0.240	21.82M
AutoML	0.188	0.72M

TABLE VI

THE LETTERS CLASSIFICATION ACCURACY OF THE PROPOSED CNNs TRAINED USING 3M SAMPLES. STN - SPATIAL TRANSFORM NET. ALX - ALEXNET. AUTOML - MNIST OPTIMIZED BY A GENETIC ALGORITHM.

Table VII and Fig. 11 list and depict the most misclassified Characters, and the most common misclassifications for each Character. It follows that the misclassified characters are indeed visually similar, and might be difficult to distinguish even for a human observer. Hence the need to utilize the sequential information using LSTM.

B. OCR results using AutoML CNN+LSTM

Following the results of Section IV-A, we studied refining the performance of the AutoML-based CNN by

L	Cand #1	Cand #2	Cand #3
נ	כ - 0.70% (64%)	ל - 0.17% (15.3%)	ד - 0.08% (7.2%)
מ	ס - 0.86% (80%)	ה - 0.19% (17.3%)	ז - 0.01% (1.0%)
ס	ק - 0.79% (84%)	ה - 0.06% (6.4%)	ש - 0.02% (2.7%)
ז	ע - 0.56% (77%)	ש - 0.05% (7.1%)	מ - 0.03% (4.8%)
ה	ת - 0.39% (62%)	מ - 0.12% (18.2%)	א - 0.08% (12.2%)

TABLE VII
THE MOST CONFUSED CHARACTERS AND THEIR MISCLASSIFICATIONS, WHEN APPLYING THE AUTOML CNN, WITHOUT THE USE OF LSTM OR BOOK-SPECIFIC REFINEMENT.

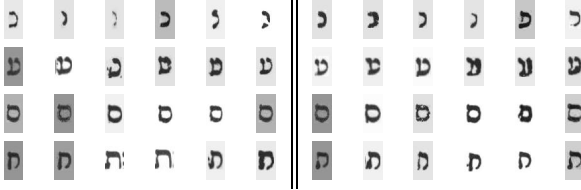


Fig. 11. The most misclassified characters. First row: נ ('nun') vs. כ ('kaf'). Second Row: מ ('tet') vs. ע ('ain') Third row: ס ('smk') vs. ק ('mem-p'). Fourth row: ז ('tav') vs. א ('het')

adding a LSTM layer to the AutoML CNN to learn the *Letters* sequences. For that we considered three training strategies. First, we "froze" the CNN weights, (L1 in Fig. 7) and trained only the LSTM layer. Denote this CNN as AutoML-LSTM. Second, we further refined the AutoML-LSTM network, by unfreezing its CNN weights (L1 in Fig. 7) and "freezing" the LSTM and FC layers (L2 and L3) and denoted the resulting network RE-CNN. Last, we refined the AutoML-LSTM CNN by training the entire network (L1+L2+L3 in Fig. 7), and denoting the resulting network RE-BOTH.

Figure 12 reports the classification error of the three schemes, and compares them to the CNN-only schemes discussed in Section IV-A. It follows that the AutoML-LSTM scheme significantly outperforms all other training variations, and the CNN-only schemes.

Table VIII reports the *Letters* accuracy results using CNN+LSTM. The confusion between נ and כ ('nun' and 'kaf'), was improved from 0.74% to 0.67% for the CNN and LSTM, respectively.

L	Cand #1	Cand #2	Cand #3
נ	כ - 0.67% (62%)	ל - 0.17% (15.7%)	ד - 0.07% (6.8%)
ס	ק - 0.68% (80%)	ה - 0.08% (9.4%)	ז - 0.02% (2.9%)
מ	ע - 0.54% (76%)	ש - 0.05% (7.4%)	ז - 0.03% (4.9%)
ק	ס - 0.55% (83%)	ה - 0.09% (14.4%)	ש - 0.01% (1.1%)
ה	ת - 0.36% (60%)	מ - 0.12% (19.1%)	א - 0.08% (12.7%)

TABLE VIII
THE MOST CONFUSED LETTERS AND THEIR ERRONEOUS DETECTIONS, USING THE PROPOSED CNN + LSTM SCHEME.

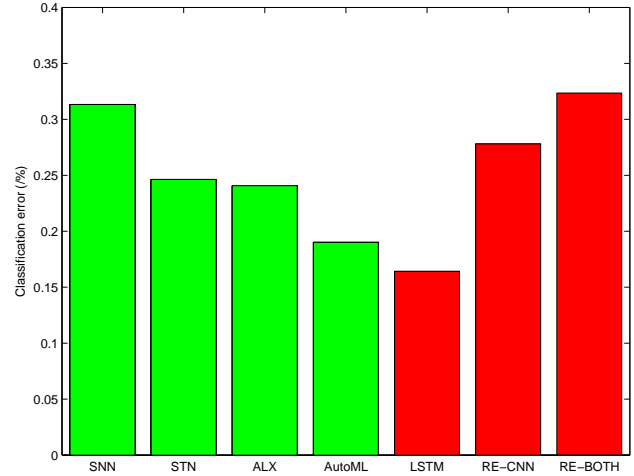


Fig. 12. Classification accuracy results of CNN+LSTM networks with different training schemes. The green bars depict the accuracy of the CNN networks. The red bars depict the further refinement of the AutoML network. LSTM : trained by training the LSTM and FC (L2+L3 in Fig. 7) layers and "freezing" the CNN layers (L1 in Fig. 7) RE-CNN: trained by "freezing" the LSTM and FC (L2+L3 in Fig. 7) layers and training the CNN layers (L1 in Fig. 7). RE-BOTH: training the entire network (L1+L2+L3 in Fig. 7).

C. Book-Specific OCR Refinement

The book-specific refinement scheme was introduced in Section III-B, allowing to utilize the invariance of the dialect of the Rashi scripts in contrast to the varying graphical manifestation of the characters. For that, given a particular *test* script (book), we applied the AutoML-LSTM CNN, trained as in Section IV-B, on a small subset of the *test* script, and used part of these *test* results, to refine the AutoML-LSTM CNN.

Thus, for each test script we applied both the CNN layers (L1 in Fig. 7) of AutoML-LSTM, and the entire AutoML-LSTM (L1+L2+L3 in Fig. 7). The characters that were classified similarly by both schemes were used as a *refinement* set for the CNN layers of AutoML-LSTM. Tables IX and X show the error classification rates of the proposed refinement scheme for the *Characters* and *Letters*, respectively. As the refinement set was relatively small, we repeated the experiment four times.

It follows that the proposed refinement scheme reduces the *Letters* classification error of the AutoML CNN+LSTM scheme from 0.188% (in Table VI) to 0.164 (in Table X), exemplifying the validity of the proposed scheme. We note that the refinement parameters corresponding to the highest *Characters* classification error (0.611% in Tables IX), do not correspond to the highest letters classification accuracy (0.164% in Tables X). We attribute that, as in Section IV-A, to the similarity

of some of the *Characters* in both Rashi and Printed scripts, resulting in *Characters* misclassifications, but accurate *Letters* classifications.

#letters	# Refinement epochs					
	1	2	5	10	20	40
1000	0.646	0.669	0.682	0.699	0.713	0.732
2000	0.636	0.674	0.688	0.693	0.692	0.706
5000	0.611	0.650	0.677	0.694	0.691	0.680
10000	0.628	0.653	0.630	0.641	0.633	0.634

TABLE IX

CHARACTERS ERROR RATE PERCENTAGE WHEN APPLYING A BOOK-SPECIFIC REFINEMENT SCHEME FOR THE AUTOML-BASED CNN+LSTM NETWORK. THE ERROR RATES ARE AVERAGES OVER 14 BOOKS. THE ERROR RATE FOR CHARACTERS WITHOUT THE PROPOSED BOOK-SPECIFIC REFINEMENT WAS 0.696%

#letters	# Refinement epochs					
	1	2	5	10	20	40
1000	0.194	0.194	0.187	0.183	0.181	0.180
2000	0.187	0.181	0.179	0.174	0.174	0.164
5000	0.184	0.176	0.175	0.171	0.166	0.164
10000	0.184	0.180	0.180	0.174	0.175	0.173

TABLE X

LETTERS ERROR RATE PERCENTAGE WHEN APPLYING A BOOK-SPECIFIC REFINEMENT SCHEME FOR THE AUTOML-BASED CNN+LSTM NETWORK. THE ERROR RATES ARE AVERAGES OVER 14 BOOKS. THE AVERAGE ERROR RATE FOR LETTERS *without* LSTM AND BOOK-SPECIFIC REFINEMENT WAS 0.188%. THE LETTERS ERROR RATE WITHOUT BOOK-SPECIFIC REFINEMENT WHILE USING LSTM WAS 0.174%

Tables VIII and XI, report the classification errors of the most confused letters, with and without the book-specific refinement, respectively. The classification errors of most letters were improved, while the accuracy of the letters ד and מ ('smk' and 'mem-p') was not. The refinement scheme improves the CNN phase, and the visual inference, while ד and מ are difficult to distinguish visually.

L	Cand #1	Cand #2	Cand #3
ג	כ - 0.42% (49%)	ל - 0.18% (21.3%)	י - 0.08% (8.9%)
ד	מ - 0.65% (84%)	ה - 0.05% (6.4%)	פ - 0.02% (2.6%)
ט	ע - 0.48% (74%)	ש - 0.05% (7.9%)	צ - 0.03% (5.3%)
ק	ס - 0.71% (89%)	ה - 0.06% (7.9%)	ב - 0.01% (0.9%)
ת	ה - 0.32% (63%)	א - 0.08% (15.2%)	ג - 0.06% (11.0%)

TABLE XI

THE MOST CONFUSED LETTERS AND THE CORRESPONDING ERRONEOUS CLASSIFICATIONS OF THE CNN+LSTM+BOOK-SPECIFIC REFINEMENT SCHEME.

We show qualitative misclassification results in Table XII, where some of the misclassification (examples 1, 2, 4, 5, and 14) are due to printing errors, while others (examples 6, 7 and 12) are due to paper erosion. Some of the misclassifications (3, 9, 10, 11 and 13) are quite similar visually and difficult to distinguish even by a human observer.

	True	False	Letter	ROI
1	א (alf)	כ (kaf)	כ	
2	ב (bet)	א (alf)	א	
3	ב (bet)	ג (gml)	ג	
4	ב (bet)	כ (kaf)	כ	
5	ב (bet)	מ (mem-p)	מ	
6	ג (gml)	נ (nun)	נ	
7	ד (dlt)	ו (vav)	ו	
8	ה (hea)	ב (bet)	ב	
9	ה (het)	ת (tav)	ת	
10	ט (tet)	ע (ain)	ע	
11	ט (tet)	ע (ain)	ע	
12	ל (lmd)	י (yod)	י	
13	מ (mem)	ע (ain)	ע	
14	נ (nun-p)	נ (nun)	נ	

TABLE XII

REPRESENTATIVE EXAMPLES OF THE MISCLASSIFICATIONS, OF THE CNN+LSTM+BOOK-SPECIFIC REFINEMENT SCHEME. THE SYMBOL IN QUESTION IS SHOWN IN THE THIRD COLUMN, AND THE CORRESPONDING ROI EXTRACTED FROM THE MANUSCRIPT IS SHOWN IN THE RIGHT COLUMN.

D. Implementation issues

The CNN (L1 in Fig. 7) and the LSTM (L2 + L3 in Fig. 7) layers of the proposed scheme were trained and implemented using the Keras wrapper [34] for TensorFlow [35]. The proposed AutoML refinement scheme introduced in Section III-A, that is based on a Genetic Algorithm, was implemented in Matlab and MatConvNet [36]. All of the training was conducted on Titan X Maxwell and the training of the AutoML CNN required four hours.

V. CONCLUSIONS

In this work we proposed a Deep Learning based approach for the OCR of manuscripts printed in the Rashi and Printed Hebrew scripts. For that, we studied and compared four CNN architectures. In particular, we learn both the characters visual appearance and the (apriori unknown) vocabulary using CNNs and LSTM, respectively. We derive an AutoML scheme based on Genetic Algorithm to optimize the CNN architecture with respect to the classification accuracy. The resulting CNN is shown to compare favourably with other CNNs based on larger (AlexNet) or similar nets. We also propose a book-specific approach for refining the

OCR CNN per book. The resulting scheme is shown to significantly outperform similar nonoptimized CNNs and achieves OCR accuracy of 99.840%.

OCR is a particular example of the Structured Image Classification problem that has multiple applications in computer vision [28] and medical imaging [29]. In future we aim to further develop and apply the proposed AutoML and book-specific refinement schemes in that context.

REFERENCES

- [1] A. Negi, C. Bhagvati, and B. Krishna, "An ocr system for telugu," in *Proceedings of Sixth International Conference on Document Analysis and Recognition*, pp. 1110–1114, 2001.
- [2] S. Dutta, N. Sankaran, K. P. Sankar, and C. V. Jawahar, "Robust recognition of degraded documents using character n-grams," in *2012 10th IAPR International Workshop on Document Analysis Systems*, pp. 130–134, March 2012.
- [3] C. V. Jawahar, M. N. S. S. K. P. Kumar, and S. S. R. Kiran, "A bilingual ocr for hindi-telugu documents and its applications," in *Seventh International Conference on Document Analysis and Recognition, 2003. Proceedings.*, pp. 408–412 vol.1, Aug 2003.
- [4] H. Bay, A. Ess, T. Tuytelaars, and L. Van Gool, "Speeded-up robust features (surf)," *Comput. Vis. Image Underst.*, vol. 110, pp. 346–359, June 2008.
- [5] Y. LeCun, B. Boser, J. S. Denker, D. Henderson, R. E. Howard, W. Hubbard, and L. D. Jackel, "Backpropagation applied to handwritten zip code recognition," *Neural Comput.*, vol. 1, pp. 541–551, Dec. 1989.
- [6] A. Bissacco, M. Cummins, Y. Netzer, and H. Neven, "Photoocr: Reading text in uncontrolled conditions," in *2013 IEEE International Conference on Computer Vision*, pp. 785–792, Dec 2013.
- [7] G. S. Lehal, C. Singh, and R. Lehal, "A shape based post processor for gurmukhi ocr," in *Proceedings of Sixth International Conference on Document Analysis and Recognition*, pp. 1105–1109, 2001.
- [8] E. H. B. Smith and K. Taghva, eds., *Document Recognition and Retrieval XII, San Jose, California, USA, January 16-20, 2005, Proceedings*, vol. 5676 of *SPIE Proceedings*, SPIE, 2005.
- [9] A. Mishra, K. Alahari, and C. V. Jawahar, "Top-down and bottom-up cues for scene text recognition," in *2012 IEEE Conference on Computer Vision and Pattern Recognition*, pp. 2687–2694, June 2012.
- [10] A. Graves, M. Liwicki, S. Fernandez, R. Bertolami, H. Bunke, and J. Schmidhuber, "A novel connectionist system for unconstrained handwriting recognition," *IEEE Transactions on Pattern Analysis and Machine Intelligence*, vol. 31, pp. 855–868, May 2009.
- [11] C. D. Santos and B. Zadrozny, "Learning character-level representations for part-of-speech tagging," in *Proceedings of the 31st International Conference on Machine Learning (ICML-14)* (T. Jebara and E. P. Xing, eds.), pp. 1818–1826, JMLR Workshop and Conference Proceedings, 2014.
- [12] Y. Kim, Y. Jernite, D. Sontag, and A. M. Rush, "Character-aware neural language models," in *Proceedings of the Thirtieth AAAI Conference on Artificial Intelligence, AAAI'16*, pp. 2741–2749, AAAI Press, 2016.
- [13] M. Jaderberg, K. Simonyan, A. Vedaldi, and A. Zisserman, "Synthetic data and artificial neural networks for natural scene text recognition," *arXiv preprint arXiv:1406.2227*, 2014.
- [14] M. Jaderberg, K. Simonyan, A. Vedaldi, and A. Zisserman, "Reading text in the wild with convolutional neural networks," *arXiv preprint arXiv:1412.1842*, 2014.
- [15] Q. Li, W. An, A. Zhou, and L. Ma, "Recognition of offline handwritten chinese characters using the tesseract open source ocr engine," in *2016 8th International Conference on Intelligent Human-Machine Systems and Cybernetics (IHMSC)*, vol. 02, pp. 452–456, Aug 2016.
- [16] S. D. Budiwati, J. Haryatno, and E. M. Dharma, "Japanese character (kana) pattern recognition application using neural network," in *Proceedings of the 2011 International Conference on Electrical Engineering and Informatics*, pp. 1–6, July 2011.
- [17] Y. Lecun, L. Bottou, Y. Bengio, and P. Haffner, "Gradient-based learning applied to document recognition," *Proceedings of the IEEE*, vol. 86, pp. 2278–2324, Nov 1998.
- [18] R. Achanta and T. Hastie, "Telugu ocr framework using deep learning.," *CoRR*, vol. abs/1509.05962, 2015.
- [19] I.-J. Kim and X. Xie, "Handwritten hangul recognition using deep convolutional neural networks," *Int. J. Doc. Anal. Recognit.*, vol. 18, pp. 1–13, Mar. 2015.
- [20] M. M. R. Sazal, S. K. Biswas, M. F. Amin, and K. Murase, "Bangla handwritten character recognition using deep belief network," in *Electrical Information and Communication Technology (EICT), 2013 International Conference on*, pp. 1–5, Feb 2014.
- [21] L. L. Ma and J. Wu, "A tibetan component representation learning method for online handwritten tibetan character recognition," in *Frontiers in Handwriting Recognition (ICFHR), 2014 14th International Conference on*, pp. 317–322, Sept 2014.
- [22] A. Sushma and V. G. S., "Kannada handwritten word conversion to electronic textual format using hmm model," in *2016 International Conference on Computation System and Information Technology for Sustainable Solutions (CSITSS)*, pp. 330–335, Oct 2016.
- [23] Z. Zhong, L. Jin, and Z. Xie, "High performance offline handwritten chinese character recognition using googlenet and directional feature maps," *CoRR*, vol. abs/1505.04925, 2015.
- [24] A. Krizhevsky, I. Sutskever, and G. E. Hinton, "Imagenet classification with deep convolutional neural networks," in *Advances in Neural Information Processing Systems 25* (F. Pereira, C. J. C. Curran, L. Bottou, and K. Q. Weinberger, eds.), pp. 1097–1105, Curran Associates, Inc., 2012.
- [25] C. Szegedy, W. Liu, Y. Jia, P. Sermanet, S. E. Reed, D. Anguelov, D. Erhan, V. Vanhoucke, and A. Rabinovich, "Going deeper with convolutions," *CoRR*, vol. abs/1409.4842, 2014.
- [26] M. Mathew, A. K. Singh, and C. V. Jawahar, "Multilingual ocr for indic scripts," in *2016 12th IAPR Workshop on Document Analysis Systems (DAS)*, pp. 186–191, April 2016.
- [27] E. Gur and Z. Zelavsky, "Retrieval of rashi semi-cursive handwriting via fuzzy logic," in *2012 International Conference on Frontiers in Handwriting Recognition*, pp. 354–359, Sept 2012.
- [28] E. Goldman and J. Goldberger, "Structured image classification from conditional random field with deep class embedding," *CoRR*, vol. abs/1705.07420, 2017.
- [29] A. Bar, L. Wolf, O. B. Amitai, E. Toledano, and E. Elnekave, "Compression fractures detection on ct," vol. 10134, pp. 10134 – 10134 – 8, 2017.
- [30] M. Jaderberg, K. Simonyan, A. Zisserman, and k. kavukcuoglu, "Spatial transformer networks," in *Advances in Neural Information Processing Systems 28* (C. Cortes, N. D. Lawrence, D. D. Lee, M. Sugiyama, and R. Garnett, eds.), pp. 2017–2025, Curran Associates, Inc., 2015.
- [31] B. Shi, X. Wang, P. Lv, C. Yao, and X. Bai, "Robust scene text recognition with automatic rectification," *CoRR*, vol. abs/1603.03915, 2016.
- [32] S. Hochreiter and J. Schmidhuber, "Long short-term memory," *Neural Computation*, vol. 9, no. 8, pp. 1735–1780, 1997.
- [33] M. Mitchell, *An Introduction to Genetic Algorithms*. Cambridge, MA, USA: MIT Press, 1998.
- [34] F. Chollet *et al.*, "Keras." <https://github.com/fchollet/keras>, 2015.
- [35] M. Abadi, A. Agarwal, P. Barham, E. Brevdo, Z. Chen, C. Citro, G. S. Corrado, A. Davis, J. Dean, M. Devin, S. Ghemawat,

- I. Goodfellow, A. Harp, G. Irving, M. Isard, Y. Jia, R. Jozefowicz, L. Kaiser, M. Kudlur, J. Levenberg, D. Mané, R. Monga, S. Moore, D. Murray, C. Olah, M. Schuster, J. Shlens, B. Steiner, I. Sutskever, K. Talwar, P. Tucker, V. Vanhoucke, V. Vasudevan, F. Viégas, O. Vinyals, P. Warden, M. Wattenberg, M. Wicke, Y. Yu, and X. Zheng, “TensorFlow: Large-scale machine learning on heterogeneous systems,” 2015. Software available from tensorflow.org.
- [36] A. Vedaldi and K. Lenc, “Matconvnet – convolutional neural networks for matlab,” in *Proceeding of the ACM Int. Conf. on Multimedia*, 2015.









ש"ס
צ"ג הש"ך
שוצת ר'
מחלוקת
ק ממונא
מסכימים
לינן צתר
וממונא,









